$$h' = h - N[1, 0, 0]\cdot[p, q, r]/[p, q, r]^2,$$
$$k' = k - N[0, 1, 0]\cdot[p, q, r]/[p, q, r]^2,$$
$$l' = l - N[0, 0, 1]\cdot[p, q, r]/[p, q, r]^2, \qquad (11)$$

where

$$[pqr] \equiv \eta_1,\ (hkl) \equiv K_2,\ hp+kq+lr = N\ .$$

This obviously embraces (3) and (9) as special cases. The formula may be proved by a slight re-adaptation of the analysis, or directly by noting that the plane $(h'k'l')$ has two properties which identify it as K_1: it contains η_1, and its intersection with K_2 is perpendicular to η_1.

As an exercise on the use of (11), we find the α-uranium K_1 corresponding to $\eta_1 = [312]$, $K_2 = (112)$:

$$h' = 1 - \frac{8[1, 0, 0]\cdot[3, 1, 2]}{9a^2+b^2+4c^2} = 1 - \frac{8\cdot 3a^2}{9a^2+b^2+4c^2}$$
$$= \frac{-15a^2+b^2+4c^2}{9a^2+b^2+4c^2},$$

$$k' = 1 - \frac{8[0, 1, 0]\cdot[3, 1, 2]}{9a^2+b^2+4c^2} = 1 - \frac{8\cdot b^2}{9a^2+b^2+4c^2}$$
$$= \frac{9a^2-7b^2+4c^2}{9a^2+b^2+4c^2},$$

$$l' = 2 - \frac{8[0, 0, 1]\cdot[3, 1, 2]}{9a^2+b^2+4c^2} = 2 - \frac{8\cdot 2c^2}{9a^2+b^2+4c^2}$$
$$= \frac{18a^2+2b^2-8c^2}{9a^2+b^2+4c^2},$$

whence $(h'k'l') = '(1\bar{7}2)'$ on eliminating the denominator and inserting numerical values for the lattice parameters a, b, c. It need hardly be stated that the corresponding reciprocal problem is also solved by (11).

Thanks are due to Dr J. D. H. Donnay for helpful advice on crystallographic terminology, and to Dr B. A. Bilby for reading the manuscript.

References

Bilby, B. A. & Christian, J. W. (1955). *Inst. Met. Monog. Rep. Series.* No. 18, p. 121.
Bullough, R. (1957). *Proc. Roy. Soc.* A, **241**, 568.
Cahn, R. W. (1953). *Acta Metallurg.* **1**, 49.
Cahn, R. W. (1954). *Advances in Physics* (*Phil. Mag. Suppl.*) **3**, No. 12.
Dove, D. B. (1956). Ph.D. Thesis, London.
Frank, F. C. (1953). *Acta Met.* **1**, 71.
Friedel, G. (1926). *Leçons de Crystallographie*, p. 436. Paris: Berger-Levrault.
Hall, E. O. (1954). *Twinning.* London: Butterworths.
Jaswon, M. A. & Dove, D. B. (1956). *Acta Cryst.* **9**, 621.
Jaswon, M. A. & Dove, D. B. (1957). *Acta Cryst.* **10**, 14.
Jaswon, M. A. (1958). *Research, Lond.* **11**, 315.
Kiho, H. (1954). *J. Phys. Soc. Japan*, **9**, 739.
Lloyd, L. T. & Chiswick, H. H. (1955). *Trans. Amer. Inst. Min.* (*Metall.*) *Engrs.* **203**, 1206.
Maruyama, S. & Kiho, H. (1956). *J. Phys. Soc. Japan*, **11**, 516.
Tertsch, H. (1949). *Die Festigkeitserscheinungen der Kristalle*, p. 56. Vienna.

Acta Cryst. (1960). **13**, 240

An Axial Retigraph

By A. L. Mackay

Birkbeck College Crystallographic Laboratory, 21, Torrington Square, London W. C. 1, England

(*Received* 14 *August* 1959)

A retigraph, an X-ray diffraction camera recording on film an undistorted projection of one plane of the reciprocal lattice of a crystal, has been constructed with some novel features. The mapping of the remainder of the reciprocal lattice on to the film plane is analysed together with other aspects of the camera geometry which also applies to the precession camera. The Lorentz and polarization corrections, both for polarized and for unpolarized incident radiation, are calculated. Methods of setting such instruments employ characteristic spots or Laue streaks.

1. Introduction

The precession camera (Buerger, 1944), which is being increasingly used for all types of crystallographic examinations, has certain drawbacks which restrict its application. The chief of these are the non-uniformity of the speed of precession (Waser, 1951), which requires the use of complicated charts for applying the Lorentz velocity-factor correction, and the long minimum specimen-to-film distance (about 50 mm.), which is much greater than the optimum for small crystals (Huxley, 1953).

An axial retigraph has been designed and constructed with the limited objective of eliminating these deficiencies. In mechanism it differs from most other retigraphs (de Jong & Bouman, 1938; Bagaryatskii & Umanskii, 1949; Kvitka & Umanskii, 1951; Torroja, Pajares & Amorós, 1951; Gay & Clastre, 1953; Rimsky, 1952) in permitting μ, the angle of precession,

and μ_1, the semi-vertical angle of the cone of reflected rays, to be indefinitely small. The retigraph of Wooster (1955) provides more facilities than does the present instrument, but at some cost in complication. Although Wooster's instrument has priority as representative of the axial type of retigraph, and operates in the radial mode also, the present instrument was designed independently of it.

2. Description of the camera

The geometrical requirements of Bragg's law are fulfilled in a straightforward way (Fig. 1). The crystal is at C with CC_0, the normal to the set of reciprocal-lattice planes under examination, inclined at an angle μ to the X-ray beam GC. The film O_1P_1 is set parallel to the reciprocal-lattice plane AC and the crystal and the film are rotated in synchronism throughout the exposure about the parallel axes CC_0 and O_1O_0 respectively. The crystal is mounted in a gimbal ring, like a two-axis universal stage, which permits any zone axis, initially lying within 30° of the axis of rotation, to be brought into coincidence with the latter. Translation to bring the crystal to the centre of rotation is accomplished by sliding the washer which carries the crystal on stiff grease. The whole crystal carrier can be transferred to the stage of a microscope for optical setting of the crystal orientation. A stationary layer-line screen SS' clips on to the back of the specimen carrier. The film plane can be advanced to record higher layers. The inclination angle μ can be varied from 0° to 30° and three specimen-to-film distances, 10, 20 and 30 mm., are present. The general scale of the instrument is chosen to take advantage of the fine-focus X-ray tube of Ehrenberg and Spear (now the Hilger tube). The actual realisation is shown in Figs. 2 and 3, the length of the box frame being about 20 cm.

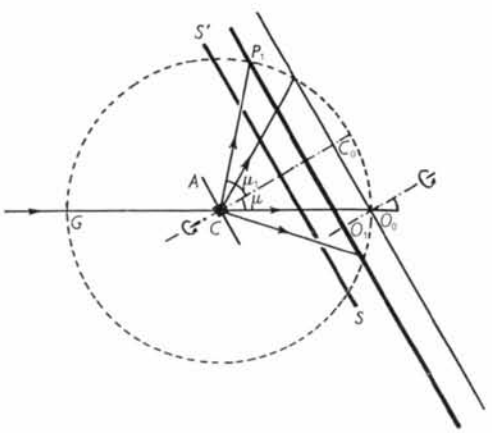

Fig. 1. The geometrical arrangement of the retigraph. GC direction of incident beam. O_1P_1 film plane, rotating about axis O_1O_0. O_1O_0 film advance for higher layers. SS' stationary layer line screen. C crystal rotating about axis CC_0. μ precession angle. μ_1 cone angle of diffracted rays.

Except for the Lorentz correction discussed in the next paragraph, the following theory applies also to the precession camera.

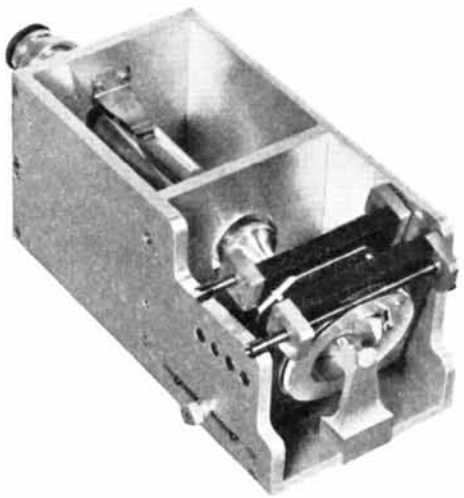

Fig. 2. General view of the retigraph. The width of the box frame is 9·5 cm. and the length 19·5 cm. The film and crystal carriers are rotated by external coupling rods from a motor which is not shown.

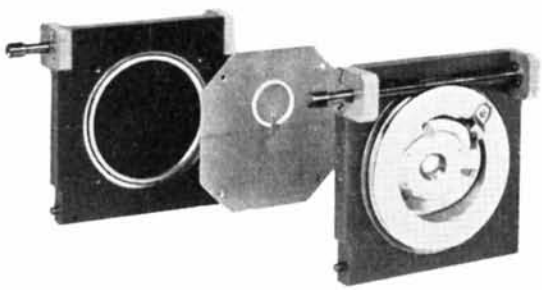

Fig. 3. Gimbal ring mounting for crystal, layer line screen and film carrier removed from the frame. This layer line screen has been replaced by an improved design which fits on to the crystal carrier. The film is 45 mm. in diameter.

3. The Lorentz (velocity) factor L

The Lorentz factor is the reciprocal of the velocity with which a reciprocal lattice point with cylindrical coordinates (ξ, φ, ζ) passes through the sphere of reflexion. ξ is measured in the reciprocal-lattice plane under examination (parallel to the film) and ζ perpendicular to it. The expression has been derived by Buerger (1944) and others.

$$1/L^2 = \xi^2 \sin^2\mu - \tfrac{1}{4}(\zeta^2 - 2\zeta\cos\mu + \xi^2)^2.$$

For an equatorial layer where $\zeta = 0$ this expression reduces to $1/L = \xi\,(\sin^2\mu - \tfrac{1}{4}\xi^2)^{\frac{1}{2}}$.

4. The polarization factor P

(*a*) The polarization factor P for an unpolarized incident beam is $P = \frac{1}{2}(1 + \cos^2 2\theta)$. Substituting $(\xi^2 + \zeta^2)^{\frac{1}{2}}$

$=2 \sin \theta$, the expression $P=1-\frac{1}{2}(\xi^2+\zeta^2)+\frac{1}{8}(\xi^2+\zeta^2)^2$ is obtained. If $\zeta=0$ (equatorial layer), $P=1-\frac{1}{2}\xi^2+\frac{1}{8}\xi^4$ as was given by Evans, Tilden & Adams (1949).

(*b*) In the present application a retigraph has been used with a bent quartz crystal monochromator as was done for the first time by Bagaryatskii (1952). In this case the polarization factor will not have the above value. It is here assumed that the axes (perpendicular to the incident beam), about which the film and the crystal planes are inclined, are in the plane containing the normals to the quartz surface, and the X-ray beams incident on and reflected from it. θ_m is the Bragg angle for reflexion from the monochromator and θ the Bragg angle for the particular reflexion under consideration. The intensity of the beam incident on the crystal (in the direction *RO* in the stereogram of Fig. 4) is $\frac{1}{2}(1+\cos^2 2\theta_m)$ divided between two plane-polarized components with vibration directions parallel to *OH* and *OV* and with amplitudes proportional to 1 and to $\cos 2\theta_m$ respectively. Each of these components must be resolved again into components in the plane of reflexion *RPAU* and in the reflecting plane *SQBW* for which the reflexion coefficients are proportional to $\cos 2\theta$ and to 1 respectively. The two initial components are phase independent so that the intensities are added, giving the total incident intensity for the vibration direction *OA* as

$$\tfrac{1}{2}(\cos^2 V\hat{O}A+\cos^2 2\theta_m.\sin^2 V\hat{O}A),$$

and for the vibration direction *OB*,

$$\tfrac{1}{2}(\sin^2 V\hat{O}A+\cos^2 2\theta_m.\cos^2 V\hat{O}A).$$

OB, *OR* and *OA* are mutually perpendicular as are *OP*, *OQ* and *OW*. $T\hat{O}V=P\hat{H}A=\mu+\mu_1-90°$. As in

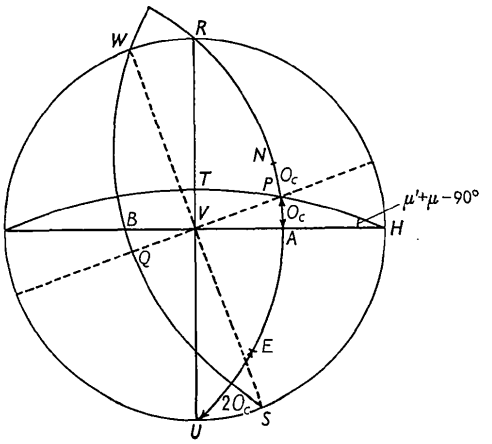

Fig. 4. Stereogram showing relationship of incident and reflected beams to camera and crystal positions. The centre of the reference sphere is denoted by *O*. *RO* incident beam from monochromator or collimator. *OH* horizontal axis about which film and crystal are tilted through the angle μ. *OV* vertical direction. *OE* beam emerging to film. *SQBW* reflecting plane with normal *OP*. *RPAU* plane of reflexion.

ΔPAH $\sin A\hat{O}H=-\tan\theta.\tan(\mu+\mu_1)$,
$\cos V\hat{O}A=-\tan\theta.\tan(\mu+\mu_1)$.

Substituting $\sin\theta=\frac{1}{2}d^*=\frac{1}{2}(\xi^2+\zeta^2)^{\frac{1}{2}}$, the expression for P reduces to

$$P=\tfrac{1}{2}+\tfrac{1}{8}\cos^2 2\theta_m.(2-d^{*2})^2 +\tfrac{1}{8}d^{*4}(\cos^2 2\theta_m-1).\tan^2(\mu+\mu_1).$$

For unpolarized radiation $\cos 2\theta_m=1$ and P reduces to the expression obtained above. Whittaker (1953) has examined the same question but has expressed the result differently. The correction for the introduction of the monochromator is numerically of the order of 10%. It will be noted that neither L nor P depends on φ.

5. Geometry of the camera

Fig. 5 shows how the reciprocal lattice of the crystal under examination, described by cylindrical coordinates (ξ, φ, ζ), is related to the possible film positions in the retigraph where the positions of the diffraction effects are described by coordinates (Ξ, Φ, Z). CO_c is 1 r.l.u. and CO_o is the actual specimen-to-film-axis distance in the retigraph (in the present instrument 10, 20 or 30 mm.). Because the reciprocal lattice has no natural scale ($d^*=\lambda/d$ and is dimensionless), but is only subject to the condition that its origin must lie in the X-ray beam and that its orientation is fixed by the crystal orientation, then, if the $Z=0$ film plane of the camera is maintained parallel to the $\zeta=0$ plane of the reciprocal lattice by the mechanism of the camera, for all purposes the reciprocal lattice can be considered as actually having its origin at O_0, the origin of the film coordinates. Hence on a scale in which the specimen film-axis distance CO_0 is 1 unit of length, the reciprocal lattice coordinates can be applied directly to the effects in the film space. In normal use the camera geometry is

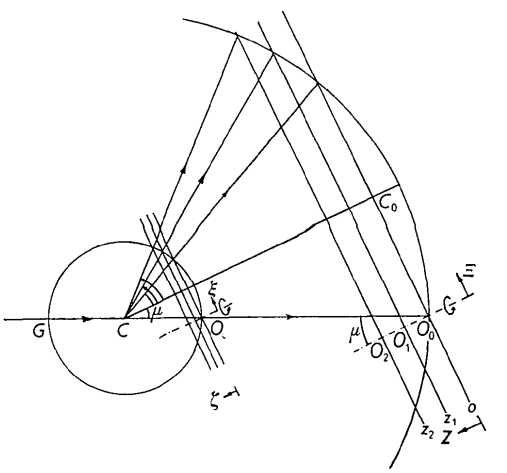

Fig. 5. Projection of the reciprocal lattice on to the film. Small circle—sphere of reflexion. *C*—crystal. Large circle—concentric sphere through centre of film.

arranged so that one layer of the reciprocal lattice is projected in undistorted form on to the film and all other layers are excluded by the layer-line screen.

The limits of the reciprocal lattice which can be recorded (Fig. 1) are given by $\xi_{max.}=\sin\mu+\sin\mu_1$, $\xi_{min.}=$radius of blind spot$=\sin\mu_1-\sin\mu$ and $\zeta_{max.}=\cos\mu-\cos\mu_1$; the practical maximum of μ_1 is about 60°, of ζ about 0·5 r.l.u. and of ξ about 1·2 r.l.u.

If a is the distance of the layer-line screen from the crystal, w the mean radius of the annular slit in the screen and δw the width of the slit, then $w=a\tan\mu_1$ and $\delta w=a\sec^2\mu_1.\delta\mu_1$. The thickness of the layer of reciprocal space which will be recorded with a slit of finite width is therefore

$$\delta\zeta=\sin\mu_1.\delta\mu_1=(\delta w/a)\sin\mu_1.\cos^2\mu_1 \\ =(\delta w/w)\sin^2\mu_1.\cos\mu_1 .$$

6. Diffraction from points with a range of ζ values

In metals where oriented precipitation has taken place, and in other circumstances, there may be diffraction effects which do not lie in the layers of the reciprocal lattice with integral indices but occur, perhaps as streaks, between ordinary lattice points.

Suppose that the X-ray film is set to record a layer of the reciprocal lattice with coordinate $\zeta=\zeta_1$ and is accordingly advanced a distance proportional to ζ_1. Because of the finite width of the layer line screen slit, points with coordinates near to ζ_1 will also be recorded on the film, but as the film advance is not correct for them, distortions will occur, that is, points P_2 and P_1 with coordinates (ξ, φ, ζ_2) and (ξ, φ, ζ_1) will not be recorded in the same place on the film. P_1 will be recorded correctly and the position in which P_2 will project on to the film must be examined. If there is no layer-line screen considerable differences in ζ may be recorded. Analytic expressions for the relations between the reciprocal lattice and film coordinates can be constructed but they are complicated and it is more satisfactory to use a semi-geometric approach.

It is easiest to analyse the geometry by taking the reciprocal lattice (film space) to be stationary. The crystal (the source of the scattered X-ray beams) will then move round a circle $AB'A'B$ (Fig. 6) of radius $\sin\mu$ and any rays passing through P_2 will lie in the surface of the corresponding cone with its apex at P_2. This cone intersects the planes $\zeta=\zeta_1$ and $\zeta=0$ in circles. The diffraction effects from a point at P_2 will, therefore, be recorded on a film in the plane $\zeta=\zeta_1$ somewhere on the circle indicated. The Bragg condition will be satisfied only when P_2 is passing through the sphere of reflexion, that is, when

$$QP_2=1.(QP_2)^2=(P_2O_2-RO_c)^2+(O_cO_2)^2+(QR)^2 \\ =(\xi-\sin\mu.\cos\Psi)^2+(\cos\mu-\zeta_2)^2+(\sin\mu.\sin\Psi)^2$$

which gives

$$\cos\Psi=(\xi^2+\zeta_2^2-2\zeta_1\cos\mu)/(2\xi\sin\mu) .$$

The radius r_1 of the circle in the ζ_1 plane is

$$(\zeta_2-\zeta_1)\sin\mu/(\cos\mu-\zeta_2)$$

and the centre of the circle is displaced a distance

$$\delta_1=\xi(\zeta_2-\zeta_1)/(\cos\mu-\zeta_2)$$

radially from the point P_1. For $\mu=30°$, $\xi=0{\cdot}75$, $\zeta_2=0{\cdot}20$, $\zeta_1=0{\cdot}10$, $\Psi=69°\,58'$, $r_1=0{\cdot}075$ and $\delta_1=0{\cdot}113$.

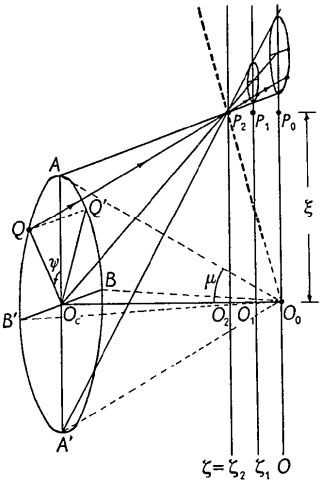

Fig. 6. Clinographic projection of stationary reciprocal lattice. With respect to this lattice the centre from which the X-rays diverge (the crystal), moves round a circle $AB'A'B$. The lattice point P_2 will be recorded when it passes through the sphere of reflexion, i.e. when $QP_2=1$ and $Q'P_2=1$. AO_0 is the crystal to film-axis distance$=1$. $AO_c=\sin\mu$.

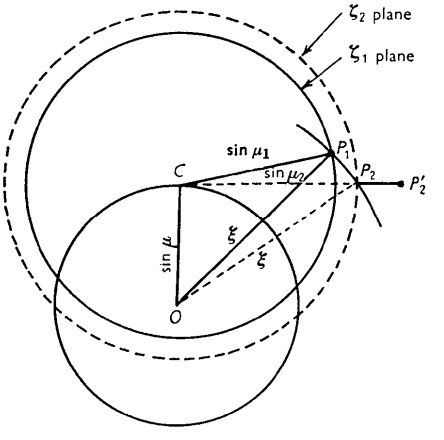

Fig. 7. Section of sphere of reflexion by plane ζ_1 (full line) superimposed on a section by the plane ζ_2. The crystal lies perpendicularly below C.

An alternative analysis is shown in Fig. 7. Here the circles represent superimposed sections of the stationary sphere of reflexion by the plane $\zeta=\zeta_1$ (solid

line) and $\zeta = \zeta_2$ (dotted line). The film is in the ζ_1 plane and the point $P_1(\xi, \varphi, \zeta_1)$ is recorded as it passes through the circle of reflexion. The circle of reflexion in the ζ_2 plane is larger and the crystal and film must rotate further until P_2 reflects. P_2 will then be directly below P_1 but because the rays are incident on the ζ_2 plane at an angle μ_2 the actual intersection with the ζ_1 plane will be at a distance $(\zeta_2 - \zeta_1) \tan \mu_2$ further from the centre of the circle. Using this construction, the way in which the lines $\xi = 0{\cdot}75$, $0{\cdot}50$ and $0{\cdot}25$, $\varphi =$ constant are recorded in the $\zeta = 0$ plane is shown in Fig. 8. It will be noted that these lines intersect and that therefore the identification of a pair of spots from measurements of their separation and distance from the centre of the film is not unique.

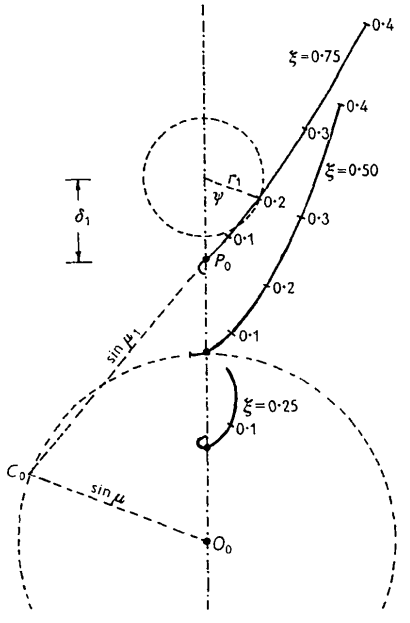

Fig. 8. Representations of the traces of the lines $\xi = 0{\cdot}75$, $0{\cdot}50$ and $0{\cdot}25$, $\varphi =$ constant, on the plane $\zeta = 0$, for $\mu = 30°$.

In any two-dimensional representation of three-dimensional data there is uncertainty which further data are needed to dispel. Only a series of sections can provide a full picture of the reciprocal lattice. Two films at $\zeta = \zeta_2$ and $\zeta = \zeta_1$ can easily be taken simultaneously to trace the plane in which the pair of reflexions due to each reciprocal-lattice point coalesces, and it might even be possible to employ cosmic ray technique with a block of lightly loaded emulsion to explore the reciprocal lattice completely.

7. Laue streaks

An algebraic treatment of the shape of the Laue streaks recorded with a range of wavelengths is complicated but a qualitative geometric description will be sufficient. In Fig. 6 a point such as P_2 representing a characteristic reflexion is superimposed on a line extending along O_0P_2 from a point $(\lambda_{\text{min.}}/\lambda_{\text{char.}})P_2O_0$ from O_0 to a distance $(\lambda_{\text{max.}}/\lambda_{\text{char.}})P_2O_0$. $\lambda_{\text{max.}}$ is about 3 Å and $\lambda_{\text{min.}}$ about 0·4 Å so that if Cu radiation is used the streak extends from $\frac{1}{3}$ the distance of P_2 to twice its distance. If the streak is in the $\zeta = 0$ plane then it will be recorded as a straight line but in the general case it can be plotted from a diagram such as Fig. 8 by taking a series of points such that $\xi = k\zeta$. In general, the streaks will be petal-shaped loops if recorded in the $\zeta = 0$ plane or loops each with a cross-over point if recorded on a higher plane $\zeta = \zeta_1$. The cross-over will occur at the wavelength λ for which $\lambda\zeta_2 = \lambda_{\text{char.}}\zeta_1$. The pair of characteristic spots will, in every case, be superimposed on the Laue streak. If it is possible to find the wavelength for which the crossover on the Laue streak occurs, by using the characteristic wavelengths of other lines occurring in the spectrum of the radiation, for example, then the ζ_2 coordinate of the spot P_2 can be estimated.

8. Stereoscopic pairs

The ultimate in film-recording X-ray cameras would be one which could record a large part of reciprocal space by a stereoscopic pair of diffraction photographs. This method of display would show Guinier–Preston zones and other complex diffraction effects most clearly. However, the previous sections have shown that, although spots do have a parallax proportional to their distance from the recording plane, their displacement is not purely radial, and they are, moreover, doubled. The doubling can be removed by closing half of the layer line screen aperture, but the displacement can only be made radial by making $\Psi = 0°$ or 180°, which is impossible for a range of points, or by making μ (and therefore r_1) very small. This last alternative opens the possibility of making stereo pairs of small volumes of the reciprocal lattice, not necessarily only near the origin, and may be applicable to the examination of constellations in reciprocal space.

9. Setting a crystal on the retigraph

(*a*) The whole plate carrying the gimbal-ring mount and the mechanism for rotating the latter can conveniently be removed to a microscope stage where the crystal can be oriented optically. This is the normal preliminary to an X-ray examination. The permanent microscope on the camera is also available for setting, particularly when an acicular crystal is to be set to rotate about its axis. Angular deviations can be read from the μ-scale on the side of the instrument.

(*b*) The normal X-ray method of setting is that described by Fisher (1952) and uses the circle of Laue streaks (from the zero layer) formed when the crystal is rotated with a small precession angle near a zone axis. Ordinary Laue photographs are also suitable for setting.

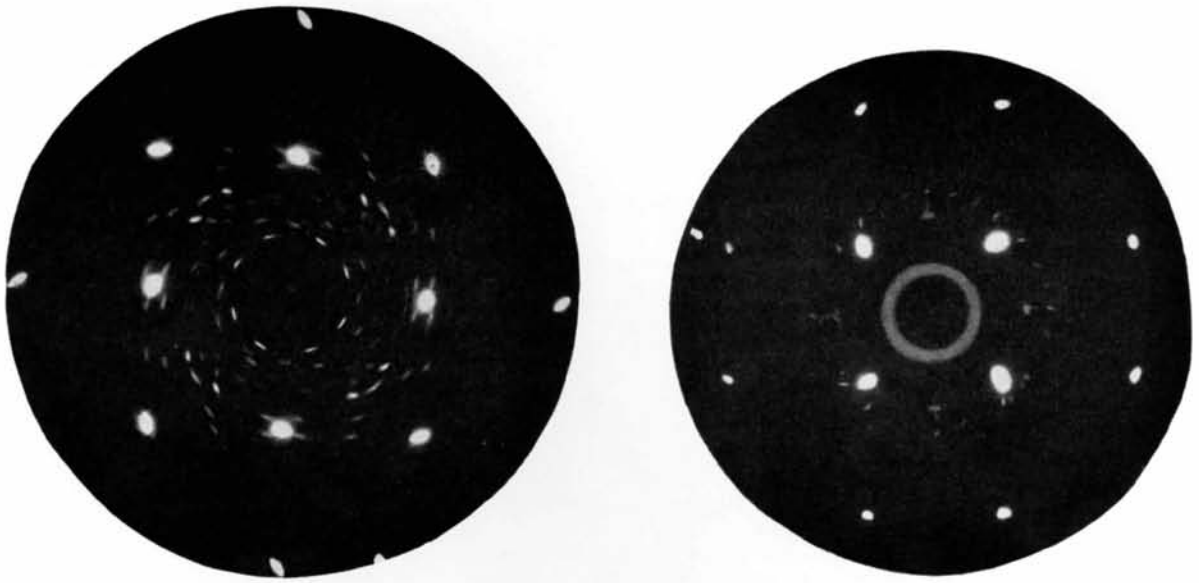

(*a*) (*b*)

Fig. 9. Diffraction photographs taken with the retigraph from an aluminium alloy crystal showing precipitation of a new phase. (Mo $K\alpha$ radiation, monochromatised, half of layer line screen obscured). (*a*) $hk0$ reflexions of aluminium matrix. (*b*) $hk1$ reflexions of aluminium matrix.

(*c*) If monochromatic radiation is used then the Laue techniques become inapplicable and recourse must be made to the results of section (6) above. When the reciprocal-lattice point lies exactly in the plane for which the camera is set it produces a single spot on the film; otherwise it will be doubled. Setting is always carried out on a zero-layer where there will be another point related by the centre of symmetry. Some estimate of the correction necessary to ζ can be made from Fig. 8. The spots on the negative ζ side will be much nearer to the correct positions. Fig. 9 shows an example of the precipitation of a new phase (small spots) in an aluminium matrix (large spots).

The construction of the instrument described was made possibly by a grant from the Central Research Fund of the University of London. The author is grateful to Miss J. M. Silcock for useful discussions on the camera and for providing the photographs of Fig. 9.

References

Bagaryatskii, Yu. A. (1952). *Dokl. Akad. Nauk SSSR*, **87**, 397.

Bagaryatskii, Yu. A. & Umanskii, M. M. (1949). *Zav. Lab.* **15**, 1320.

Buerger, M. J. (1944). *The photography of the reciprocal lattice. ASXRED.*

Evans, H. T., Tilden, S. G. & Adams, D. P. (1949). *Rev. Sci. Instrum.* **20**, 150.

Fisher, D. J. (1952). *Amer. Min.* **37**, 1036.

Gay, R. & Clastre, J. (1953). *J. Phys. Radium*, **14**, 535.

Huxley, H. E. (1953). *Acta Cryst.* **6**, 457.

Jong, W. F. de, & Bouman, J. (1938). *Zeit. Kristallogr.* **98**, 456.

Kvitka, S. S. & Umanskii, M. M. (1951). *Zav. Lab.* **17**, 174.

Rimsky, M. (1952). *Bull. Soc. Franc. Min. Crist.* **75**, 500.

Torroja, J. M., Pajares, E. & Amorós, J. L. (1951). *J. Sci. Instrum.* **28**, 44.

Waser, J. (1951). *Rev. Sci. Instrum.* **22**, 563.

Whittaker, E. J. W. (1953). *Acta Cryst.* **6**, 222.

Wooster, W. A. (1955). *Acta Tech. Hungarica*, **12**, 165.